J. Fluid Mech. (1974), *vol.* 63, *part* 4, *pp.* 753–763
Printed in Great Britain

The stability of a trailing line vortex. Part 1. Inviscid theory

By MARTIN LESSEN,
Department of Mechanical and Aerospace Sciences,
University of Rochester, New York 14627

PAWAN JIT SINGH
Institute for Fundamental Studies, Department of Physics,
University of Rochester, New York 14627

AND FREDERICK PAILLET
Department of Mechanical and Aerospace Sciences,
University of Rochester, New York 14627

(Received 14 May 1973 and in revised form 28 November 1973)

The inviscid stability of swirling flows with mean velocity profiles similar to that obtained by Batchelor (1964) for a trailing vortex from an aircraft is studied with respect to infinitesimal non-axisymmetric disturbances. The flow is characterized by a swirl parameter q involving the ratio of the magnitude of the maximum swirl velocity to that of the maximum axial velocity. It is found that, as the swirl is continuously increased from zero, the disturbances die out quickly for a small value of q if $n = 1$ (n is the azimuthal wavenumber of the Fourier disturbance of type $\exp\{i(\alpha x + n\phi - \alpha ct)\}$); but for negative values of n, the amplification rate increases and then decreases, falling to negative values at q slightly greater than 1·5 for $n = -1$. The maximum amplification rate increases for increasingly negative n up to $n = -6$ (the highest mode investigated), and corresponds to $q \simeq 0{\cdot}85$. The applicability of these results to attempts at destabilizing vortices is briefly discussed.

1. Introduction

Various phenomena associated with swirling flows have been studied for at least a century; such flows are of increasingly great interest considering present concern with aircraft trailing vortices, vortical transport of momentum and energy in meteorology, and vortex bursting. However, as was demonstrated by Hoffman & Joubert (1963), the presence of a swirling component of velocity makes analysis by usual dimensional arguments extremely difficult. For this reason, few solutions to the equations of motion for swirling flows, either turbulent or laminar, have been made available for use in a generalized stability analysis.

The study of the stability of shearing and rotating flows, treated as separate and distinct problems, began with the now famous work of Lord Rayleigh. Each of the two general problems has since been formulated in great detail for many different mean velocity profiles and flow situations, and useful results obtained. However, attempts at superimposing the two types of flows with their fundamentally different types of instability have been made only recently. Considering the analogy which may be drawn between density stratification and rotation, Howard & Gupta (1962) tried to find a stability criterion analogous to that involving the Richardson number developed by Miles and Howard for stratified flows. Uberoi, Chow & Narain (1972) studied the stability of a coaxial rotating jet and vortex in the approximation of long and short wavelengths. The discontinuous or non-smooth velocity profiles used in their analysis are a simple if crude representation of actually measured profiles. Widnall & Bliss (1971) studied the motion and stability of a vortex filament containing an axial flow in the limit of slender-body theory. Lessen, Deshpande & Hadji-Ohanes (1973) investigated the stability of similar profiles by computing numerically the growth rates for a large range of wavenumbers.

In the present study, the inviscid stability of a simple axisymmetric wake with superimposed swirling flow is investigated. Only non-axisymmetric disturbances are considered since the analysis of Howard & Gupta (1962) implies that the role of stable swirl is purely stabilizing for axisymmetric disturbances, while the wake alone is already stable with respect to such axisymmetric disturbances. The difficulty in relating the stability of the mean flow profiles assumed for this study to that of the vortex system trailing from the edge of a lifting surface is readily admitted; however, the analysis seeks to determine the fundamental way in which the distributions of rotation and axial shear interact to determine the stability of such a swirling wake. (It will appear from our results that the interaction mechanism described in Pedley (1969) is of probable importance.) The stability of the far wake region is considered in the same spirit as that in which the Bickley jet and other far-field similarity profiles have been used in previous stability studies. The similarity laws which govern the far wake region will determine the shape of the mean velocity profiles, while the relative intensity of the swirl and axial velocity defect can be controlled by external means. This means that the stability behaviour will be a function of this relative intensity (characterized by a swirl parameter q defined in the next section). The particular swirling far wake under study is obtained by superimposing the Lamb (1932, p. 592) profile for a convecting and diffusing vortex upon the ordinary axisymmetric far-wake profile. That such a situation is consistent with the fluid equations suitably far downstream and at high free-stream Reynolds numbers is indicated in the analysis of trailing line vortices by Batchelor (1964).

2. Formulation of the problem

Batchelor's similarity solution for a swirling wake flow is given by

$$W = \frac{1-e^{-\eta}}{r_0} C_0, \quad \eta = \frac{U_0 r_0^2}{4\nu x}, \tag{1}$$

$$U = U_0 - \frac{C_0^2}{8\nu x} \log \frac{U_0 x}{\nu} e^{-\eta} + \frac{C_0^2}{8\nu x} Q(\eta) - L \frac{U_0^2}{8\nu x} e^{-\eta}, \tag{2}$$

where U and W are the axial and azimuthal velocity profiles respectively, U_0 is the free axial velocity, ν is the kinematic viscosity, x is the axial distance from some origin, C_0 is the constant circulation at large radius r_0, L is a constant depending on the induced drag or the initial velocity defect in the presimilarity stage, and

$$Q(\eta) = e^{-\eta}\{\log \eta + \mathrm{ei}(\eta) - 0{\cdot}807\} + 2\mathrm{ei}(\eta) - 2\mathrm{ei}(2\eta), \tag{3}$$

where

$$\mathrm{ei}(\eta) = \int_\eta^\infty \frac{e^{-y}}{y}\,dy.$$

It can be shown that the third term on the right-hand side of (2), involving $Q(\eta)$, is much smaller than the second term, particularly at large free-flow Reynolds numbers $Re = U_0 x/\nu$ characterizing the similarity region; for the purposes of this study, this term is disregarded.

The stability problem is formulated by deriving the well-known linearized momentum and continuity perturbation equations, and then Fourier analysing the velocity and the pressure perturbation. If u', v', w' are the axial, radial and azimuthal components of the velocity perturbation respectively and p' is the pressure perturbation, one can write

$$\{u', v', w', p'\} = \{F, iG, H, P\}(r_0)\exp\{i(\alpha x + n\phi - \alpha ct)\}, \tag{4}$$

where α and n are axial and azimuthal wavenumbers, $c = c_r + ic_i$ is the complex phase velocity, ϕ is the azimuthal co-ordinate and F, G, H and P are the complex amplitudes of the perturbation. The above quantities have been non-dimensionalized with respect to a velocity scale U_s and length scale r_s, where

$$U_s = \frac{C_0^2}{8\nu x}\log\frac{U_0 x}{\nu} + L\frac{U_0^2}{8\nu x}, \tag{5}$$

$$r_s = (U_0^2/4\nu x)^{\frac{1}{2}}, \tag{6}$$

which also transforms (1) and (2) to non-dimensional mean velocity profiles U and W as follows:

$$W = q\frac{(1-e^{-r^2})}{r^2}, \quad q = \frac{C_0}{U_s r_s}, \quad U = \frac{U_0}{U_s} - e^{-r^2}, \quad r = \frac{r_0}{r_s}.$$

It can be shown that translation and inversion of the axial velocity profile only affects the frequency and does not alter the amplification factor c_i. Thus, we shall use $U = e^{-r^2}$ as the mean axial velocity distribution. Figure 1 illustrates the shape of the axial and tangential profiles; the maximum value of W occurs at $r = 1{\cdot}122$ and equals $0{\cdot}639q$. If q' is the ratio of the maximum swirl velocity to the maximum axial velocity, $q' = 0{\cdot}639q$.

The perturbation equations in terms of F, G, H and P are as follows:

$$[nW/r + \alpha(U-c)]F + U'G = -\alpha P, \tag{7}$$

$$[nW/r + \alpha(U-c]G + 2WH/r = P', \tag{8}$$

$$[nW/r + \alpha(U-c)]H + (W' + W/r)G = -nP/r, \tag{9}$$

$$\alpha F + G' + G/r + nH/r = 0. \tag{10}$$

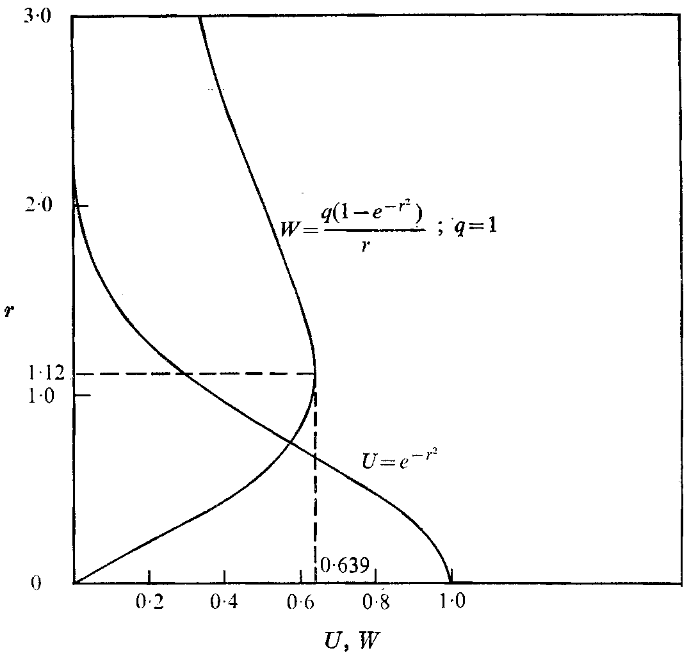

FIGURE 1. The axial and tangential mean velocity profiles U and W respectively.

The boundary conditions, requiring that F and P do not depend on ϕ at $r = 0$ and all the quantities be finite, are given by

$$\left.\begin{aligned} &G(0) = H(0) = 0, \quad F(0), P(0) \text{ finite for } n = 0,\\ &G(0) \pm H(0) = 0, \quad F(0) = P(0) = 0 \text{ for } n = \pm 1,\\ &G(0) = H(0) = F(0) = P(0) = 0 \text{ for } |n| > 1,\\ &G(\infty) = H(\infty) = F(\infty) = P(\infty) = 0 \text{ for all } n. \end{aligned}\right\} \tag{11}$$

Equations (7)–(10) can be reduced to a single second-order equation and such a reduction, as obtained by Howard & Gupta also, yields

$$\gamma^2(SG^*)' - \left[\gamma^2 + \gamma r\left\{S\left(\frac{\gamma'}{r} + \frac{2nW}{r^3}\right)\right\}' - \frac{2\alpha WS}{r^2}(\alpha\gamma W^* - nU')\right]G = 0, \tag{12}$$

where $$\gamma = \alpha(U-c) + \frac{nW}{r}, \quad S = \frac{r^2}{n^2+\alpha^2r^2}$$

and a prime and an asterisk denote the operators d/dr and $d/dr + 1/r$ respectively. The following transformation of the dependent variable simplifies the equation:

$$Z = \gamma G/r.$$

Equation (12) then reduces to

$$\begin{aligned} &r^2\gamma^2(n^2+\alpha^2r^2)Z'' + [(n^2-\alpha^2r^2)r\gamma^2 + 2(n^2+\alpha^2r^2)r^2\gamma\gamma']Z' \\ &- [\gamma^2(n^2+\alpha^2r^2)^2 + 2(n^2+\alpha^2r^2)nr\gamma(W/r)' - 4n\alpha^2r\gamma W \\ &- 2\alpha W(n^2+\alpha^2r^2)(\alpha(rW)' - nU')]Z = 0. \end{aligned} \tag{13}$$

This equation along with the boundary conditions $Z(0) = Z(\infty) = 0$ constitutes an eigenvalue problem. As a timewise stability problem, we shall attempt to determine c as an eigenvalue for given values of α and q; the disturbances are amplified or damped with time depending upon whether $c_i > 0$ or $c_i < 0$ respectively. $c_i = 0$ characterizes neutral disturbances.

3. Procedure

Equation (13) is regularly singular near $r = 0$ (assuming that $\gamma(0) \neq 0$; if this is not true, the equations must be handled differently). Thus, a Frobenius power-series solution near $r = 0$ can be obtained; its radius of convergence will depend upon the zeros of γ. The roots of the indicial equation are $\pm n$. U and W are expanded in power series in r and the coefficients of the series are numerically computed by programming the recursive relations.

The asymptotic solutions valid for large r can also easily be determined. As r becomes large, $U \to 0$ and $W \to q/r$ asymptotically. For this potential vortex velocity distribution (7)–(10) reduce to Bessel's equation in F whose solution valid at large r is the modified Bessel function $K_n(\alpha r)$. It can be shown that $G = -F'/\alpha$, and since $Z = rG/\gamma$ the asymptotic solution for Z is $-ArK_n'(\alpha r)/\gamma$, where a prime again denotes differentiation with respect to r only, and A is an arbitrary constant. The ratio Z'/Z is found to be

$$\frac{Z'}{Z} = \frac{K_n''}{K_n'} + \frac{1}{r} + \frac{2nq}{nqr - \alpha c r^3}. \tag{14}$$

Starting with these asymptotic values, the solution of (13) is advanced towards $r = 0$ by numerical integration and then matched to the known Frobenius series solution at some fixed radius near zero. If Z_n and Z_n' are the values of Z and its derivative at some small radius r_F obtained by numerical integration, and Z_F and Z_F' are the corresponding values known from the power series, the matching of the solutions yields the dispersion relation

$$F(\alpha, n, c, q) = \begin{vmatrix} Z_n & Z_F \\ Z_n' & Z_F' \end{vmatrix} = Z_n Z_F' - Z_n' Z_F = 0. \tag{15}$$

The zeros of F for given values of α, n and q are the eigenvalues c.

An additional difficulty is associated with the zeros of the factor $\gamma(r)$ which multiplies the higher derivatives in (13) and (15). This problem is related to the limiting process associated with infinite Reynolds numbers, and with the derivation of the second-order inviscid equations from the sixth-order set of three-dimensional viscid disturbance equations. Using vector notation, the full set of equations may be transformed into the following set of six first-order equations:

$$\epsilon Z_i = \sum_{k=0}^{\infty} A_{ij}^{(k)} \epsilon^k Z_j \quad (i, j = 1, 2, 3, 4, 5, 6),$$

where $\epsilon = (iRe)^{-\frac{1}{2}}$. Use of the asymptotic technique given by Wasow (1965, p. 190) to investigate the limit $\epsilon \to 0$ at some $r = r_c$ where $\gamma(r_c) = 0$ but $\gamma'(r_c) \neq 0$ shows that the criterion developed by Lin (1955, p. 130) for the two-dimensional case can be easily extended to the case considered here. That is, the solution of the inviscid equations is rigorously valid for amplified disturbances, while the path of numerical integration may be deformed according to Lin's criterion (if the real part of $\gamma'(r_c)$ is greater than zero, the path lies below the real axis and vice versa) in cases near neutral stability to avoid the appearance of large coefficients during the integration process. Such a singular point (usually called a 'critical point') which is important in the stability of the non-swirling axisymmetric wake as investigated by Lessen & Singh (1973) is seen to occur somewhere in the flow field for all cases considered here.

4. Numerical technique

The Runge–Kutta method with Gill's modification is used to integrate the perturbation equation. The integration is carried from a large r ($r \simeq 3$, where the error in the mean velocity profile is of order 10^{-3}) to a small r ($|r| \leqslant 0{\cdot}25$ depending upon the singularities of γ), where the Frobenius solution is calculated by summing the contributions of various terms in the series, whose coefficients are numerically determined. The criterion for truncating the series is that the ratio of the contribution of the last term to the partial sum up to that term must be less than a given small number.

The sets of parameters $\{\alpha, q, n, c\}$ which satisfy the dispersion relation (15) are sought; α and q are given and the informed guesses for c_r and c_i are achieved through guidance from some known values at slightly different values of α and q for a fixed n. The Newton–Raphson method is used to achieve convergence to an accurate eigenvalue from the guessed estimate. When $q = 0$, the axial mean flow corresponds to that for a laminar wake, whose inviscid stability has already been investigated by Lessen & Singh (1973). These known eigenvalues serve as a reliable estimate as the swirl parameter q is slowly increased. The iteration is carried out until at least three-decimal-point accuracy is achieved, and normally fewer than three or four iterations are enough for this purpose.

5. Results and conclusions

This analysis was originally undertaken to investigate the stability of aircraft trailing vortices. The observed behaviour of such swirling wakes has been interpreted as the effect of a highly stable swirl distribution on the normally unstable wake. However, the presence of the vortex introduced a distinction between positive and negative azimuthal wavenumbers, and the negative ($-n$) modes are initially destabilized by the addition of swirl. This agrees with the results of Lessen *et al.* and Uberoi *et al.*, who found that the negative ($-n$) azimuthal modes are, in general, more unstable than the corresponding positive modes. For this reason, we have concentrated on the analysis of these negative modes, after illustrating the direct stabilization of the $n = +1$ mode for small values of q.

Figure 2 shows the variation of c_i and c_r with q for different α when $n = 1$, revealing that the $n = 1$ mode is stabilized by the addition of very small amounts of swirl; for this mode only, stabilization at all α occurs for a value of q lying

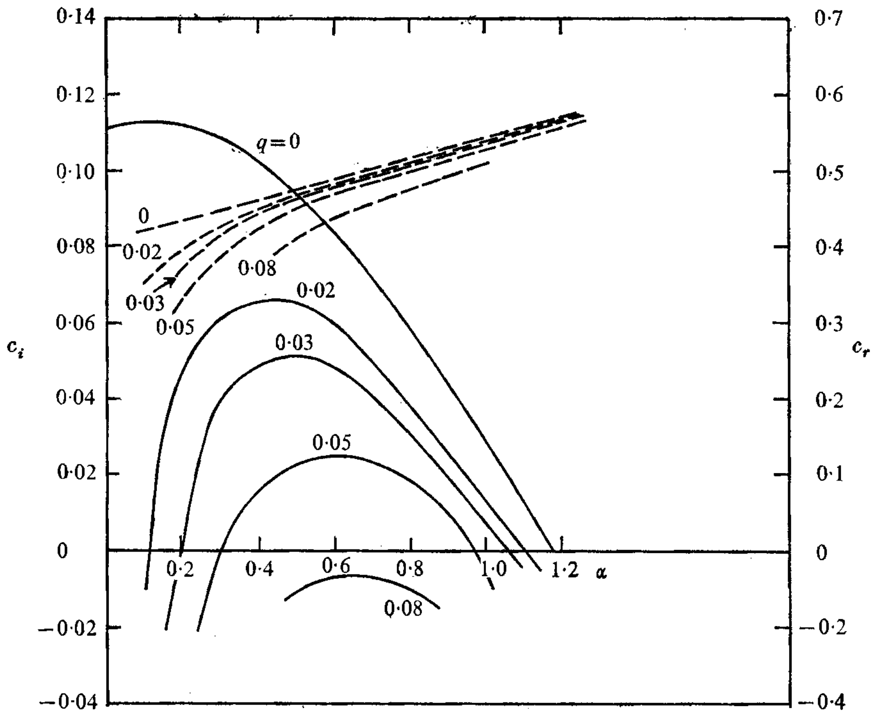

FIGURE 2. The variation of c_r (broken lines) and c_i (solid lines) with α for different values of swirl parameter q for the $n = 1$ mode.

between 0·07 and 0·08 and there is a contracting range of unstable wavenumbers as q approaches this limiting value.

The results for the negative azimuthal modes are very different. The initial superposition of a small amount of swirl leads to enhanced instability for the $n = -1$ mode, and to even greater instability for the $n \leqslant -2$ modes, which are completely stable without the swirl. The maximum growth rate (product of axial wavenumber and imaginary part of the phase speed) for each negative azimuthal mode appears to increase continuously with $|n|$. The corresponding values of α at which these maximum growth rates occur also increase continuously with $|n|$, while the associated value of q approaches approximately 0·83. Figures 3(*a*), (*b*) and (*c*) show the values of the growth rate plotted against the axial wavenumber for the lowest six negative modes (for $q = 0{\cdot}40$, 0·80 and 1·20 respectively). The maximum growth rates calculated for those modes which were investigated are listed in table 1, along with the corresponding values of α and q. Finally, all wavelengths appear to become damped, and the flow completely stabilized, at some value of q slightly greater than 1·5.

The outstanding features of the results listed are the direct stabilization of the $n = +1$ mode, the initial strong destabilization of the $-n$ modes (especially whose which are stable for the wake itself) and the eventual indication of complete stabilization for all modes at some $q > 1{\cdot}5$. The only other similar stability analysis with which to compare these results is that due to Bergman (1969) for a swirling

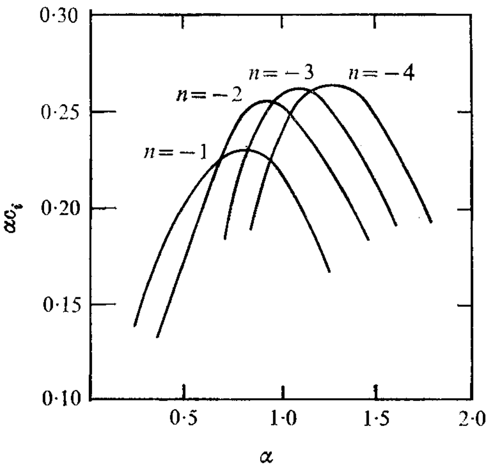

(*a*)

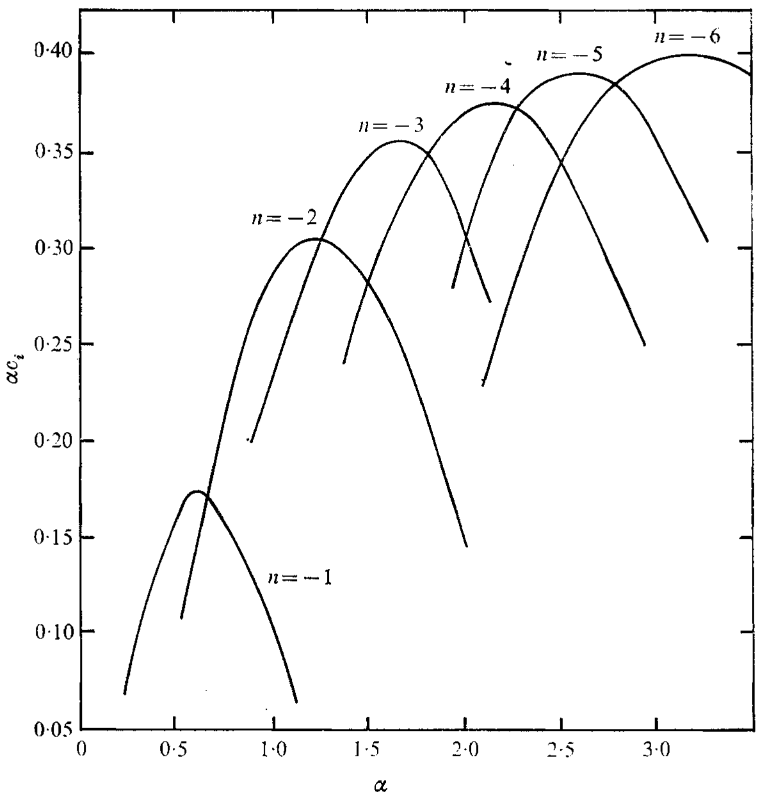

(*b*)

FIGURES 3(*a*, *b*). For legend see facing page.

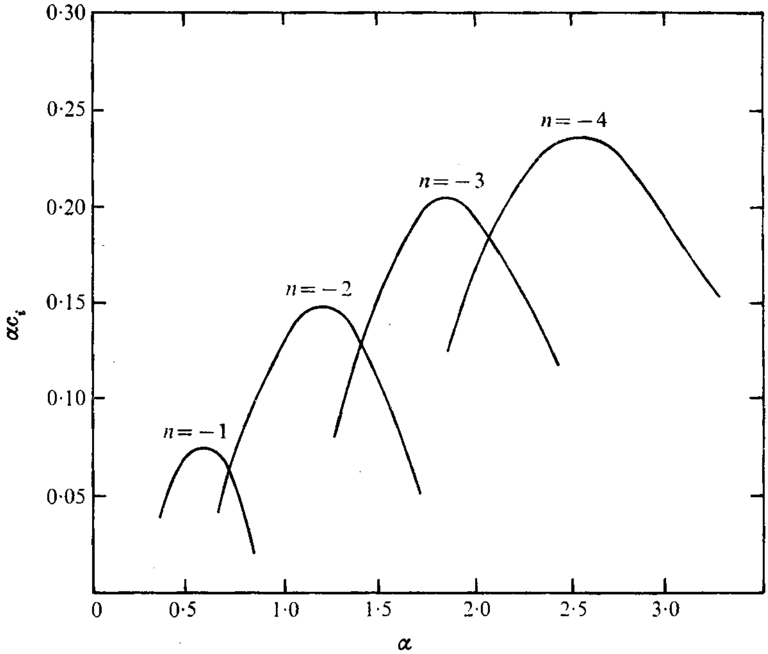

(c)

FIGURE 3. The variation of αc_i with α for (a) $q = 0{\cdot}40$ (for modes $n = -1, -2, -3, -4$), (b) $q = 0{\cdot}80$ (for modes $n = -1, -2, -3, -4, -5, -6$) and (c) $q = 1{\cdot}20$ (for modes $n = -1, -2, -3, -4$).

n	αc_i	α	q
−1	0·1470	0·3	0·32
−2	0·3138	1·2	0·70
−3	0·3544	1·7	0·79
−4	0·3777	2·15	0·82
−5	0·3912	2·6	0·83
−6	0·4008	3·2	0·83

TABLE 1

flow with somewhat similar velocity profiles. He obtained growth rates of approximately the same magnitude for the lowest unstable mode, but the instability does not disappear completely for larger values of the swirl parameter used. Also, Pedley (1968) has shown that the superposition of large solid-body rotation (itself rotationally stable) on pipe Poiseuille flow destabilizes modes that are found to be stable for the pipe flow alone. The results obtained here for moderate swirl bear such close resemblance to those obtained in Pedley's inviscid analysis that the same general mechanism (as credited to McIntyre by Pedley 1969) should be suspected. However, this case differs from the rapidly rotating pipe situation in the presence of a critical point, where

$$\gamma = \alpha(U(r)-c)+nW(r)/r = 0.$$

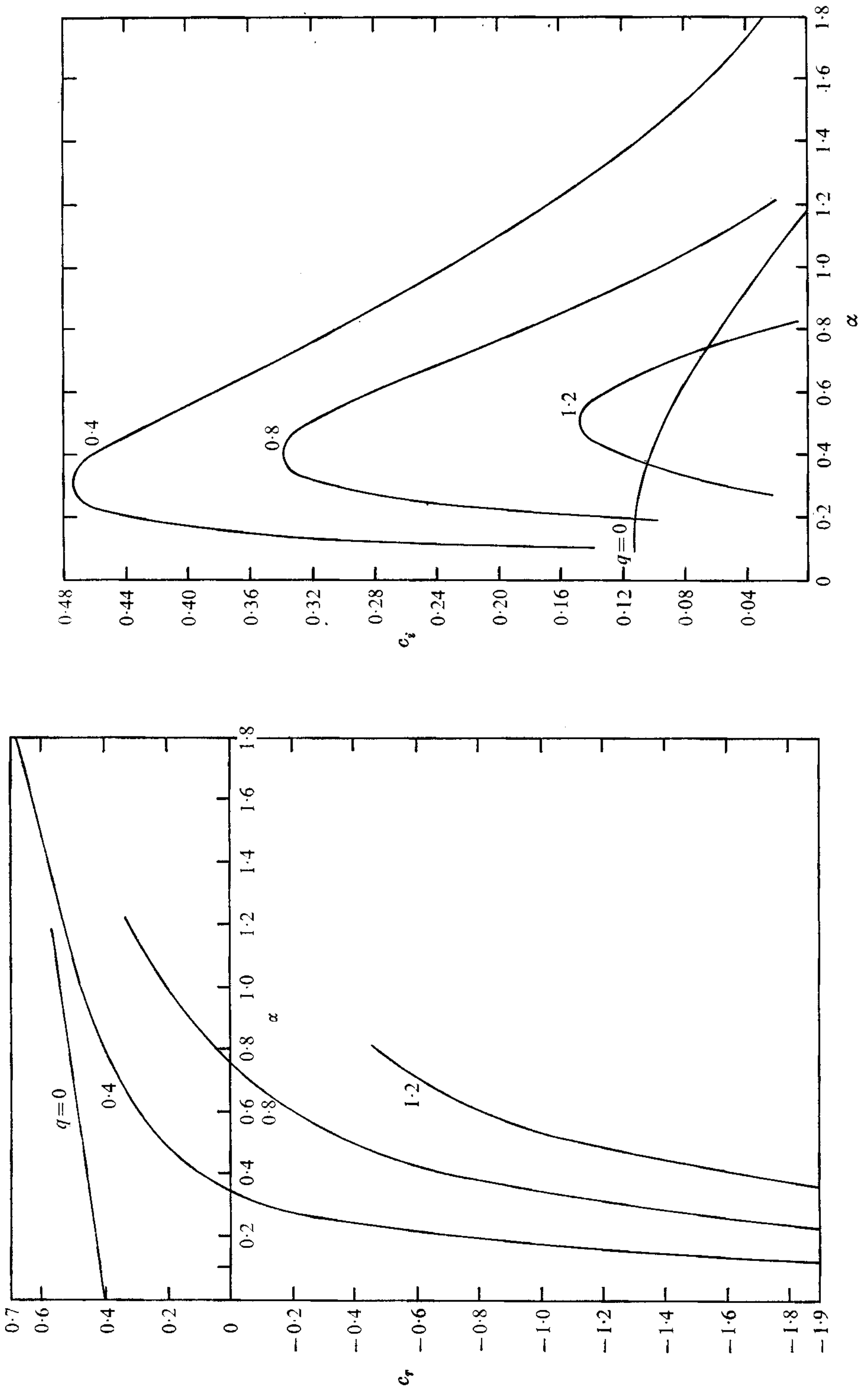

(*a*) (*b*)

FIGURE 4. The variation of (*a*) c_r and (*b*) c_i with α for various q for the $n = -1$ mode. The maximum value of c_i occurs for $q \simeq 0{\cdot}31$ (not shown in the figure).

Experience with less complicated two-dimensional parallel-flow problems suggests that the disturbance growth rates should be sensitive to the values of the mean flow quantities which occur at this point (although Pedley has shown that a critical point is not necessary for the destabilization of a stable axial flow by a stable rotation). The general behaviour of this singular point can be inferred from figures 4(*a*) and (*b*), where the real and imaginary parts of the phase speed are plotted against α for various values of q and $n = -1$. The significance of the critical point in this three-dimensional case is hard to define beyond such general statements, but the asymptotic nature of Pedley's analysis makes a detailed comparison with his treatment equally difficult.

Only the inviscid growth rates are calculated in this study. The trend towards larger wavenumbers for the $-n$ modes suggests that viscosity (or turbulent eddy transport) will interfere with these modes when α becomes too large. For this reason the first few $-n$ modes may still dominate, since they reach growth rates nearly as large as those of higher modes but at much lower values of α. This matter is now being clarified through the complete viscid analysis of the same swirling far-wake flow profile.

This work was partly supported by the National Science Foundation.

REFERENCES

BATCHELOR, G. K. 1964 Axial flow in trailing line vortices. *J. Fluid Mech.* **20**, 645.

BERGMAN, K. H. 1969 On the dynamic instability of convective atmospheric vortices. Ph.D. thesis, Dept. of Atmospheric Sciences, University of Washington.

HOFFMAN, E. R. & JOUBERT, P. N. 1963 Turbulent line vortices. *J. Fluid Mech.* **16**, 395.

HOWARD, L. N. & GUPTA, A. S. 1962 On the hydrodynamic and hydromagnetic stability of swirling flows. *J. Fluid Mech.* **14**, 463.

LAMB, H. 1932 *Hydrodynamics*, 6th edn. Dover.

LESSEN, M., DESHPANDE, N. V. & HADJI-OHANES, B. 1973 Stability of a potential vortex with non-rotating and rigid-body rotating top-hat jet core. *J. Fluid Mech.* **60**, 459.

LESSEN, M. & SINGH, P. J. 1973 The stability of axisymmetric free shear layers. *J. Fluid Mech.* **60**, 433.

LIN, C. C. 1955 *The Theory of Hydrodynamic Stability*. Cambridge University Press.

PEDLEY, T. J. 1968 On the instability of rapidly rotating shear flows to non-axisymmetric disturbances. *J. Fluid Mech.* **31**, 603.

PEDLEY, T. J. 1969 On the instability of viscous flow in a rapidly rotating pipe. *J. Fluid Mech.* **35**, 97.

UBEROI, M. S., CHOW, C. Y. & NARAIN, J. P. 1972 Stability of coaxial rotating jet and vortex of different densities. *Phys. Fluids*, **15**, 1718.

WASOW, W. 1965 *Asymptotic Expansions for Ordinary Differential Equations*. Interscience.

WIDNALL, S. E. & BLISS, D. B. 1971 Slender body analysis of the motion and stability of a vortex filament containing an axial flow. *J. Fluid Mech.* **50**, 335.